

Secondary sonic boom modelling for realistic atmospheric conditions

Philippe Blanc-Benon ^{*}, Laurent Dallois [†] and Julian Scott [‡]

Laboratoire de Mécanique des Fluides et d'Acoustique

Ecole Centrale de Lyon & UMR CNRS 5509

69134 Ecully cedex, France .

The shock waves generated by a supersonic aircraft are reflected in the upper part of the atmosphere. Back to the ground, they are indirect sonic booms called secondary sonic booms. The recorded signals of secondary sonic booms show a low amplitude and a low frequency. They sound like rumbling noises due to amplitude bursts. These signals strongly depend on the atmospheric conditions, in particular to the amplitude and to the direction of the wind in the stratopause. The propagation of the secondary sonic boom is studied using atmospheric models up to the thermosphere. By solving temporal ray equations, the secondary carpet position is investigated. An amplitude equation including nonlinearity, absorption and relaxation by various chemical species is coupled to the ray solver in order to get informations on the amplitude and on the frequency of the sonic boom at the ground level. Using this propagation model and the atmospheric model, the seasonal dependencies of the secondary sonic boom are investigated. Multipath arrivals are directly linked to wind field or 3D inhomogeneities. They have been of special concern as a way to explain the rumble noise as a summation over different ray contributions.

I. Introduction

The atmospheric sound speed profile creates waveguides for the shock waves generated by a supersonic aeroplane. The upward shock waves is reflected back to the ground by the temperature gradients in the stratopause or in the thermosphere. The resulting noise disturbance is called secondary sonic boom. It is merely an infrasonic signal and it sounds like a rumble noise associated to bursts.^{1,2} In the present work, the propagation of secondary sonic booms is studied using realistic atmospheric models up to the thermosphere. The secondary carpet position is investigated by solving temporal ray equations. An amplitude equation including nonlinearity, absorption and relaxation by various chemical species is coupled to the ray solver to obtain the secondary boom signature at the ground level. The predicted signatures are compared to recorded signals of secondary sonic booms. A good agreement is found for the amplitude and for the time duration. The bursts seem to be related to multipath arrivals due to direct and indirect secondary sonic boom. The rumbling noise can be interpreted as the effect of finer structures of the atmosphere as gravity waves.

^{*}Directeur de Recherche CNRS, philippe.blanc-benon@ec-lyon.fr

[†]Post-Doc at Ecole Centrale de Lyon, laurent.dallois@ec-lyon.fr

[‡]Professor at Ecole Centrale de Lyon, julian.scott@ec-lyon.fr

II. Theoretical background

The prediction method is based at least on two assumptions. The first one is that the atmosphere varies over length scales greater than the actual length of the supersonic boom. The second assumption is that the shocks are only weak shocks, *i.e.* the shock pressure amplitude is less than a few percent of the underlying pressure field. The model is derived from the generalized Navier-Stokes equations including earth rotation and from the state equations for the different molecular species of the atmosphere to get relaxation effects. From these equations, a two-step asymptotic development can be conducted. At the first step, a ODE system of six equations is obtained. This system provides the shock wave trajectory called boom rays. A boom ray is the trajectory of the boom generated by the supersonic aircraft at a time τ at an azimuthal angle ψ . Each ray can be parametrised by τ and ψ plus the curvilinear coordinate along the trajectory, λ . Actually, because of causality, the time t can be kept as the parameter along the ray in place of λ . The ray family generated by these q parameters is denoted by $\mathbf{X}(\tau, \psi; t)$ and the ray direction at each point is denoted by $\mathbf{k}(\tau, \psi; t)$. These both quantities, \mathbf{X} and \mathbf{k} , has to be solved together to obtain the ray paths. The Mach surface created by the aeroplane at a given time t_0 is the location of all the points $\mathbf{X}(\tau, \psi; t_0)$ and this surface is perpendicular to all the vectors $\mathbf{k}(\tau, \psi; t_0)$. It is also denoted by the relation $\Phi(\mathbf{x}, t) = 0$.

In order to access to the ray tube area which is, in first approximation, inversely proportional to the amplitude of the sonic boom, four other vectors has to be included to the resolution. They give the variations of $\mathbf{X}(\tau, \psi; t)$ and $\mathbf{k}(\tau, \psi; t)$ in accordance to the parameters τ and ψ . They are denoted by

$$\mathbf{X}_\tau = \frac{\partial \mathbf{X}}{\partial \tau}, \quad \mathbf{k}_\tau = \frac{\partial \mathbf{k}}{\partial \tau}, \quad \mathbf{X}_\psi = \frac{\partial \mathbf{X}}{\partial \psi}, \quad \text{and} \quad \mathbf{k}_\psi = \frac{\partial \mathbf{k}}{\partial \psi}.$$

The ray tube area, ν , is given by

$$\nu = |\mathbf{X}_\tau \times \mathbf{X}_\psi|. \quad (1)$$

To compute these quantities along each ray, a system of eighteen equations has to be solved. These equations are

$$\frac{d X_i}{dt} = v_{0i}(\mathbf{X}, t) + c_0(\mathbf{X}, t)n_i \quad (2)$$

$$\frac{d k_i}{dt} = - \left(\frac{\partial v_{0j}}{\partial x_i} \Big|_{\mathbf{X}} + \frac{\partial c_0}{\partial x_i} \Big|_{\mathbf{X}} n_j \right) k_j, \quad (3)$$

$$\frac{d X_{\alpha i}}{dt} = \left(\frac{\partial v_{0i}}{\partial x_j} \Big|_{\mathbf{X}} + \frac{\partial c_0}{\partial x_j} \Big|_{\mathbf{X}} n_i \right) X_{\alpha j} + c_0(\mathbf{X}, t) (\delta_{ij} - n_i n_j) \frac{k_{\alpha j}}{|\mathbf{k}|}, \quad (4)$$

$$\frac{d k_{\alpha i}}{dt} = - \left(\frac{\partial v_{0j}}{\partial x_i} \Big|_{\mathbf{X}} + \frac{\partial c_0}{\partial x_i} \Big|_{\mathbf{X}} n_j \right) k_{\alpha j} - \left(\frac{\partial v_{0j}}{\partial x_i x_k} \Big|_{\mathbf{X}} + \frac{\partial c_0}{\partial x_i x_k} \Big|_{\mathbf{X}} n_j \right) k_j X_{\alpha k}. \quad (5)$$

where α has to be replaced either by τ or by ψ . The vector \mathbf{n} is defined by $\mathbf{n} = \mathbf{k}/k$ where $k = |\mathbf{k}|$. The quantities $c_0(\mathbf{r})$ and $\mathbf{v}_0(\mathbf{r})$ are respectively the sound speed and the wind velocity of the atmosphere. It is assumed they are known data. The boom rays start at the aeroplane position at a given time τ and are parametrized by their launching angle θ , the azimuthal angle around the aeroplane. The boom rays are similar to the acoustical rays due to the weak shock assumption. The main difference is that their launching polar angle ϕ is fixed by the relation $\phi = \arccos(1/M)$ where M is the Mach number. At a given time, all the shock waves generated by the aeroplane along its trajectory are located on a surface called the Mach surface.

The second step of the development leads to an amplitude equation which must be solved along each ray. Defining ξ as $\xi = \Phi(\mathbf{x}, t)/|\nabla \Phi|_a$, where the a subscript means taken at the aircraft position, it can be used as a distance perpendicular to the Mach surface $\Phi(x, t)$ at a given time t . Thus, along a given ray and at a given time, the coordinate ξ corresponds to the location $\mathbf{X}(t) + \mathbf{n}(t)\xi/k$ in the earth cartesian referential.

If the acoustic field $\phi = (c_0/\rho_0)^{1/2}\rho'_1$ is expressed in term of this new variable ξ and the time t , an equation describing its evolution is:

$$\begin{aligned} \frac{\partial \phi}{\partial t} = & -\frac{1}{2} \left\{ \frac{\nabla \cdot (c_0^2 \mathbf{n})}{c_0} + \nabla \cdot \mathbf{v}_0 + \mathbf{n} \cdot (\mathbf{n} \cdot \nabla \mathbf{v}_0) \right\} \phi \\ & - \frac{\gamma+1}{2} k \left(\frac{c_0}{\rho_0} \right)^{1/2} \phi \frac{\partial \phi}{\partial \xi} - \Lambda k \frac{\partial \phi}{\partial \xi} + D k^2 \frac{\partial^2 \phi}{\partial \xi^2} \\ & - k \frac{\partial}{\partial \xi} \int_{-\infty}^{+\infty} g(Y) \phi(\xi + kY) dY. \end{aligned} \quad (6)$$

where Λ , D and $g(Y)$ depend on the underlying thermodynamic state at $\mathbf{x} = \mathbf{X}(t)$. Λ correspond to the sound speed variations mainly due to the difference between the frozen sound speed and the equilibrium sound speed. D is the acoustic dissipation coefficient due to viscosity, thermal conduction and diffusion. The summation into the definition of $g(Y) = -\sum_{\alpha} Z_{\alpha} G_{\alpha}(Y)$ is performed over the molecular species involved into the relaxation process. Each $G_{\alpha}(Y) = \exp(-\lambda_{\alpha} Y)$ is an eigenfunction of the linear system of the relaxation equations for the eigenvalue λ_{α} . In first approximation, the relaxation equations can be decoupled and λ_{α} corresponds to the eigenvalue of each relaxation equations.

Introducing $u = \nu^{1/2} k^{-1} \phi$ in place of ϕ into the equation (6) reduces it to:

$$\frac{\partial u}{\partial t} = D k^2 \frac{\partial^2 \rho'_1}{\partial \xi^2} - \Lambda k \frac{\partial u}{\partial \xi} - k \frac{1+\gamma}{2} \left(\frac{c_0}{\rho_0} \right)^{1/2} u \frac{\partial u}{\partial \xi} - k \frac{\partial}{\partial \xi} \int_{-\infty}^{+\infty} g(Y) u(\xi + kY) dY \quad (7)$$

So, the amplitude is proportional to k and to the inverse of the square root of ν . This include the geometrical spreading of the shock and the “stratification” effects due to the variations of the underlying atmosphere (mainly pressure and density variations). As expected, the amplitude is becoming infinite at caustic positions ($\nu = 0$) and an other asymptotic expansion as to be performed around caustic. The u function is only related to absorption, relaxation and non-linearity processes. The convection process implying by the Λ term is a displacement along the \mathbf{n} direction of the whole wave around the position given by the ray equations. Actually, it could be included to the ray equations as a low order correction. In this analysis, it has been kept into the amplitude equation even if it does not change much of the results. This equation is used to models the deformation of the shock wave during its propagation into the inhomogeneous atmosphere. It is a nonlinear paraxial equation that includes dispersion, absorption and relaxation effects. This equation is no more valid when the associated ray goes through a caustic and a Hilbert transform is then applied to the shock wave to simulate the crossing of the caustic.

III. Numerical scheme

The resolution of the sonic boom equation is a three step process. In figure 1 is plotted the scheme of the computational process. The aircraft trajectory and the atmospheric data are given parametres for the problem. The first stage is to compute a large number of boom rays for different airplane positions and different launching angles. Thus a mapping is obtained between the initial parameters of the boom rays and the location of the secondary booms. An other benefit is that allow to separate the secondary booms in different families such as direct or indirect secondary booms or rays reflected in the stratopause or in the thermosphere. From this continuous mapping, the process can be reversed to find the initial parameters which leads to the creation of a secondary sonic boom at a given earth location. This leads to the choice of one or several rays to get the secondary boom signature at a given earth latitude and longitude.

The next stage is to evaluate the ray tube area ν and the marker $\mathbf{n} \cdot \boldsymbol{\nu}$ all along these chosen rays. As explain in the part II, it is a way to find when the boom ray reaches a caustic. Each caustic is precisely located along each ray and the corresponding propagation time is kept. The first reason to this stage is

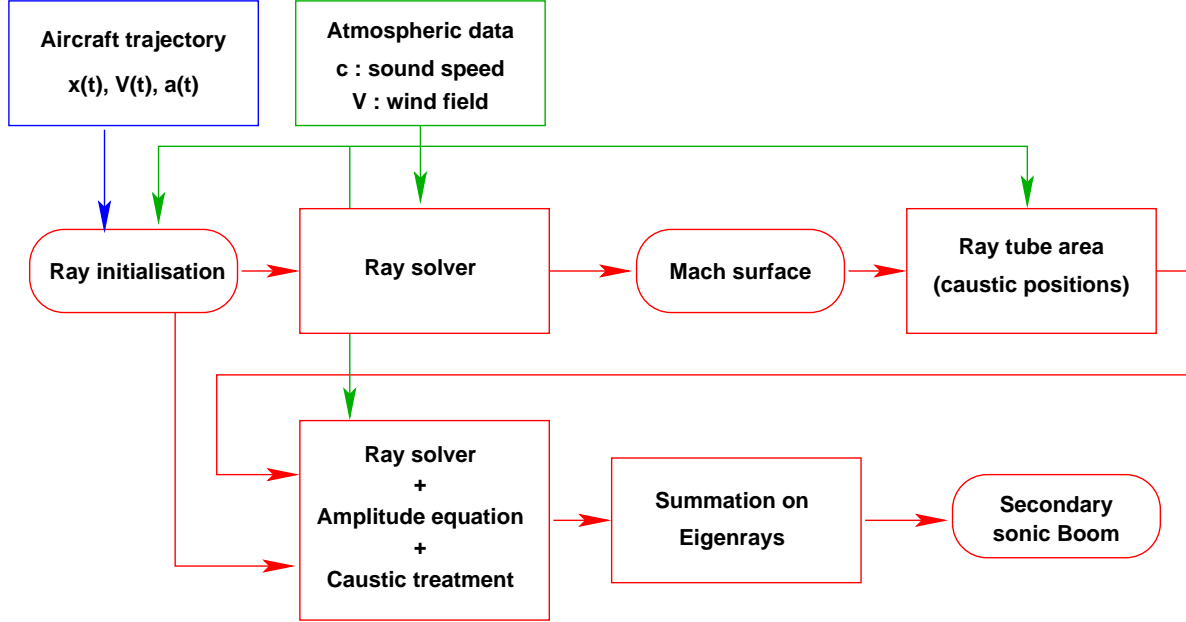


Figure 1. Process to compute secondary sonic boom signature.

to evaluate where the amplitude equation (eq. (7)) can be applied, and when the caustic model as to be applied. The second reason is to estimate how many rays must be expected at a given location. As explain in the section II, the number of rays going through a point of the space is different for each side of the caustic. The caustics correspond to a fold in the mapping linking each point of the space to the initial conditions. So, going through a caustic tends to increase the number of paths from the source (the moving aircraft) to a given location.

The last stage implied the sonic boom evolution equation (eq. (7)). Due to the singularity of the model at the aircraft location, the initial condition is imposed a few meters (400 m) away from the aircraft. A N-wave is used as the initial sonic boom signature. Its peak pressure is 400 Pa and its total length is 60 m. These are characteristic values of Concorde supersonic flight. The equation (7) is solved along each chosen rays until the ray reach a caustic. There, the amplitude computation is stopped and the evaluated signature at this point is kept as the incoming wave for the transonic model. The outgoing wave resulting of the Hilbert transform is used as the initial condition when the amplitude computation is resumed as soon as the ray leaves the transonic region.

The signature of the secondary boom for each ray should be summed in a last stage to get the real perturbation signal at a given earth location. In practice, the time delay between two contributions is much larger than the duration of an individual signature. As a result, there is no interaction between two booms propagating on different rays and the summation is useless. The smallest delay between two arrivals is around 15 s.

IV. Heigh altitude wind effects

In order to compare further case with wind profile, lets have a brief discussion on the configuration without any wind and just a vertical profile of sound speed. The using sound speed profile is characteristic from the atmospheric ones. It is plotted on the figure 2(a). As the aircraft altitude during a supersonic

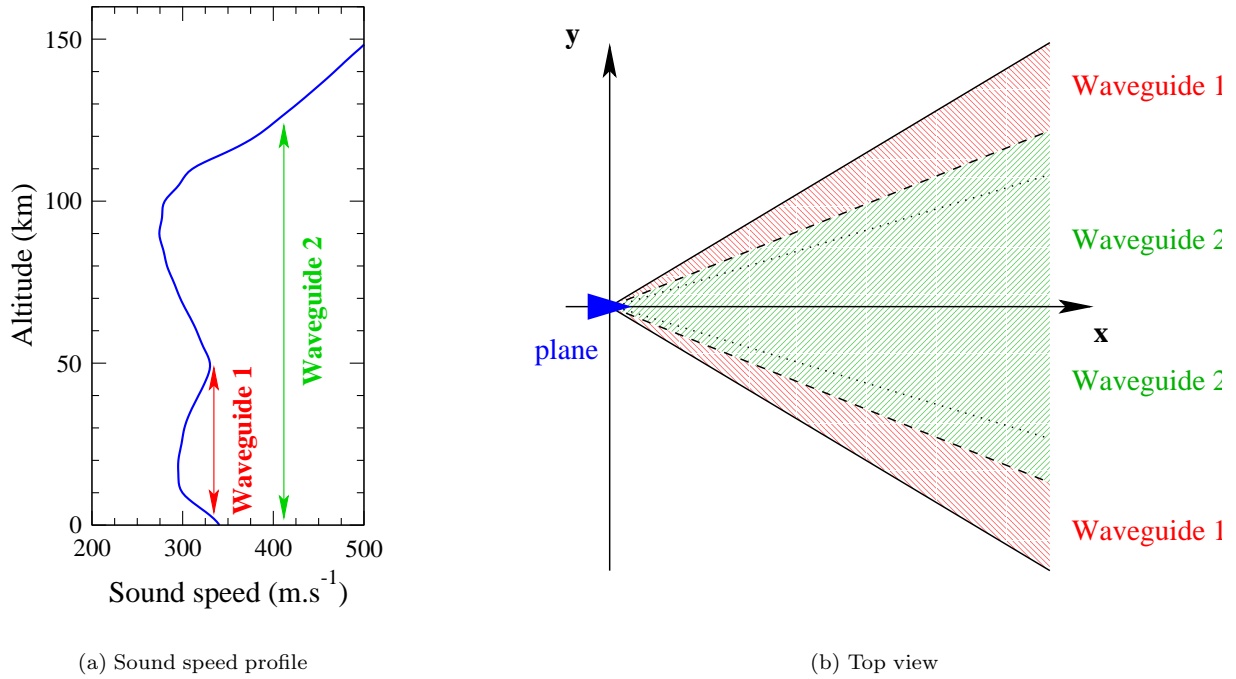


Figure 2. Atmospheric wave guides (top view).

flight is around 15 km, two waveguides are allowed to the shock rays; the stratospheric waveguide between an altitude of few kilometers up to the stratosphere (~ 50 km) and the thermospheric waveguide between the ground level and the thermosphere (above 100 km). Actually, the type of the shock ray (stratospheric or thermospheric) depends on the initial launching angle ψ and a limit angle ψ_0 . It can be summarized like this (see diagram (2(b))):

$|\psi| < \psi_0$ the shock rays is able to go through the stratospheric region and is reflected on the sound speed gradient into the thermosphere.

$|\psi| > \psi_0$ the shock rays is reflected into the stratosphere and never reaches the upper part of the atmosphere where the absorption is dominant.

Actually, an other important limit angle ψ_g is the angle above which the rays reached the ground. For an atmospheric sound speed profile, this angle is below ψ_0 , ($\psi_g < \psi_0$). This means that the only shock rays to reach the ground are the thermospheric ones and this shock rays are mostly absorbed in the upper part of the atmosphere. The figure (3) shows the Mach surface and the primary and secondary carpet position for this configuration. Actually, the whole part of the secondary, the direct and the indirect one, are created by thermospheric rays which are reflected at an altitude of 120 km. Due to their long travel into the thermosphere where absorption and relaxation are the main effects, a low amplitude wave is expected. The shock rays that are restrained to the waveguide 1 never reach the ground. The secondary Mach carpet is between 250 km and 300 km beyond the plane (here at the origin). The interval between the arrivals of the direct (first secondary carpet) and the indirect (second secondary carpet) shock ray is about 2 minutes for a ground observer at the vertical of the aircraft trajectory. This is a first occurrence of multipath arrivals.

Actually there is three crucial height regions in this problem: the troposphere (up to 15 km), the stratopause (around 50 km) and the thermosphere (over 100 km). In this part, the stratopause heights

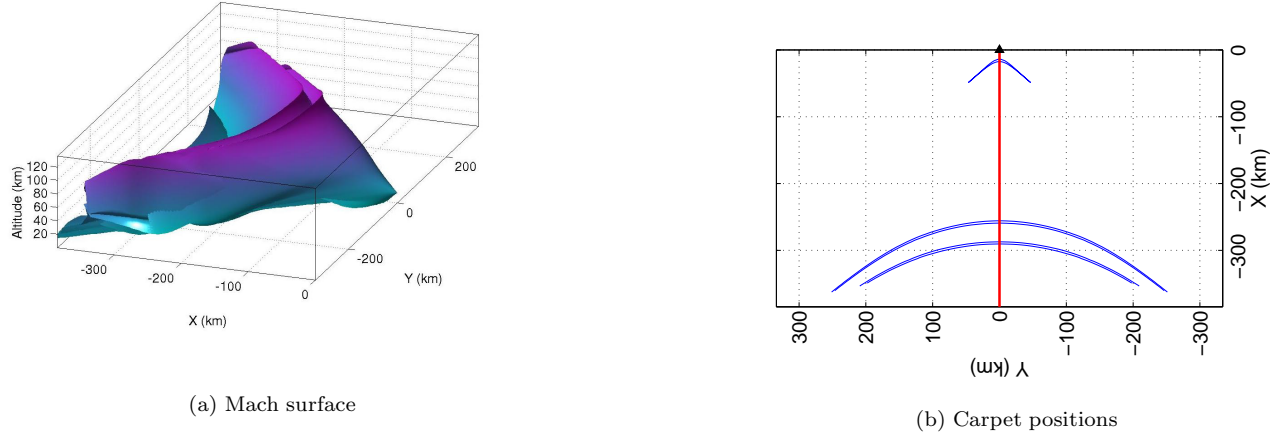


Figure 3. Configuration without any wind

are investigated by adding a vertical wind profile to the previous sound speed profile. The figure (4) shows side by side the two profiles.

The wind is distributed has a gaussian centered around the stratopause region (50 km here). This is a simple model of the atmospheric conditions during summer when a jet wind appears into the stratosphere. The main effect of the wind is to increase or to decrease the sound speed in this region depending of its direction relatively to the propagation direction of the shock. Three main cases are checked in the figure (IV): the upwind case (figure 5(a)) when the shock is propagating against the wind, the downwind case (figure 5(b)) when the shock is convected by the wind and the transverse wind (figure 5(c)) when the wind blows crosswise to the aircraft trajectory. The upwind configuration gives similar results to the ones obtained without any wind. As the wind is localized on a small region of space, it does not affect much the position of the rays and the direct and the indirect secondary carpet are mostly at the same locations than previously (see figure (3(b))).

In the downwind configuration, in addition to the secondary carpets we get in the two previous case, new carpets appear on both side of the aircraft trajectory. They are located far from the trajectory but at a lesser distance from the aircraft than the last ones. These carpets are generated by rays trapped into the waveguide 1 (see figure (2)) and reflected one or more times at the stratopause. In the upper and lower left corners are the one generated after two reflections in the upper part of the atmosphere. These carpets can be coupled together, one being created by the direct rays and the other one by the indirect rays and the. They will be called stratospheric carpets to differentiate them from the classical ones we would call thermospheric carpets. The effective sound speed into the stratopause, given by

$$c_0 + \mathbf{V}_0 \cdot \mathbf{n}$$

where \mathbf{n} is the propagation direction of the shock, is greater than the actual celerity needed by the rays to reach the ground. As these rays never reach the thermospheric region where the absorption becomes the most important effect, it can be expected to have greater shock wave amplitudes along these new carpet than along the thermospheric ones. It can be also noticed that for some ground positions, the number of secondary boom arrival increase from two to three or four, even more if we consider the ones reflected two times. The time interval between this multipath arrivals is at most 5 minutes.

The crosswind configuration is intermediate between the two other cases. The symmetry along the trajectory disappear and each side can be linked to one of the two previous case. Into the upwind side, only the thermospheric secondary carpet appear without much difference with the no wind case. Into the

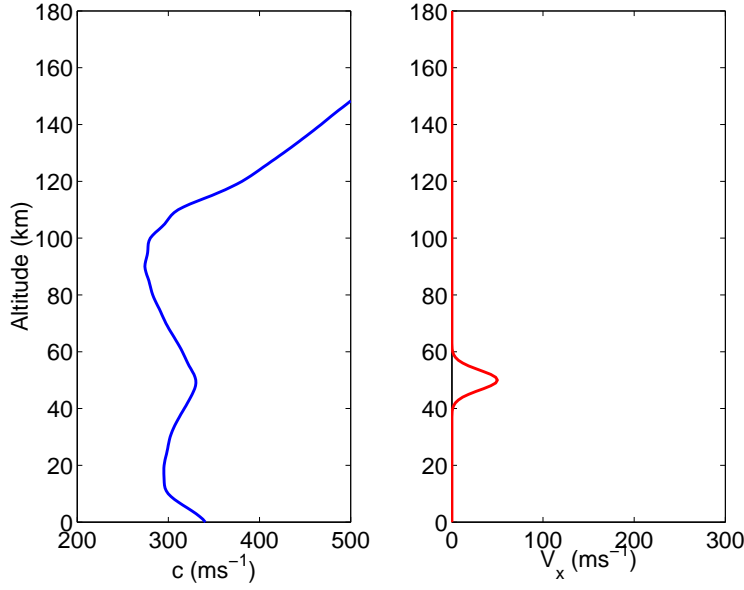


Figure 4. Sound speed and wind profile.

downwind side, the stratospheric secondary carpets are present and their positions are only slightly moving from the downwind case.

In conclusion, the occurrence of the tropospheric secondary carpets is directly related to the wind profile at the stratopause. The amplitude of the shock wave along them is certainly more important than the amplitude along the thermospheric carpet; the shock rays never reach the upper part of the atmosphere where relaxation and absorption weaken the perturbation and transform it into a very low frequency wave.

V. Atmospheric data

The model presented in the previous section has been applied to realistic atmospheric conditions. The atmospheric fields are provided by the IAP (Leibniz-Institut für Atmosphärenphysik, Universität Rostock).

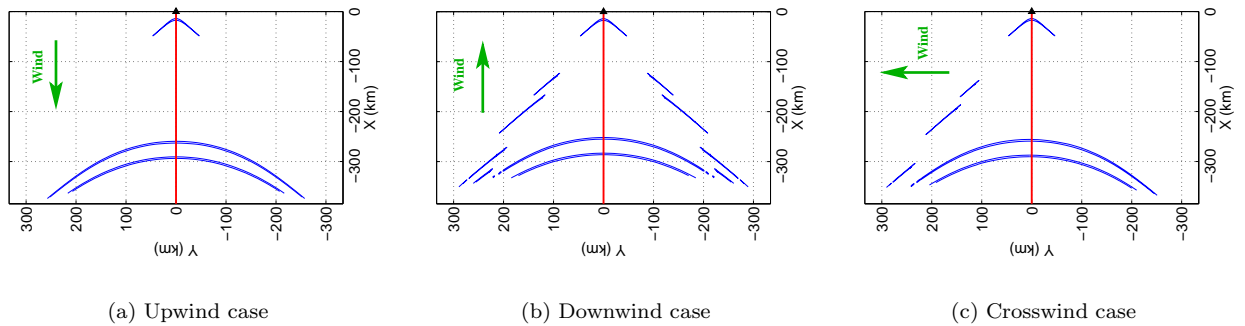


Figure 5. Influence of the direction of the wind.

They include mean pressure, density, temperature and wind data at a given latitude ($69^\circ N$) up to an altitude of 150 km. They are discretized every 10 km along the latitude and every 100 m along the altitude.

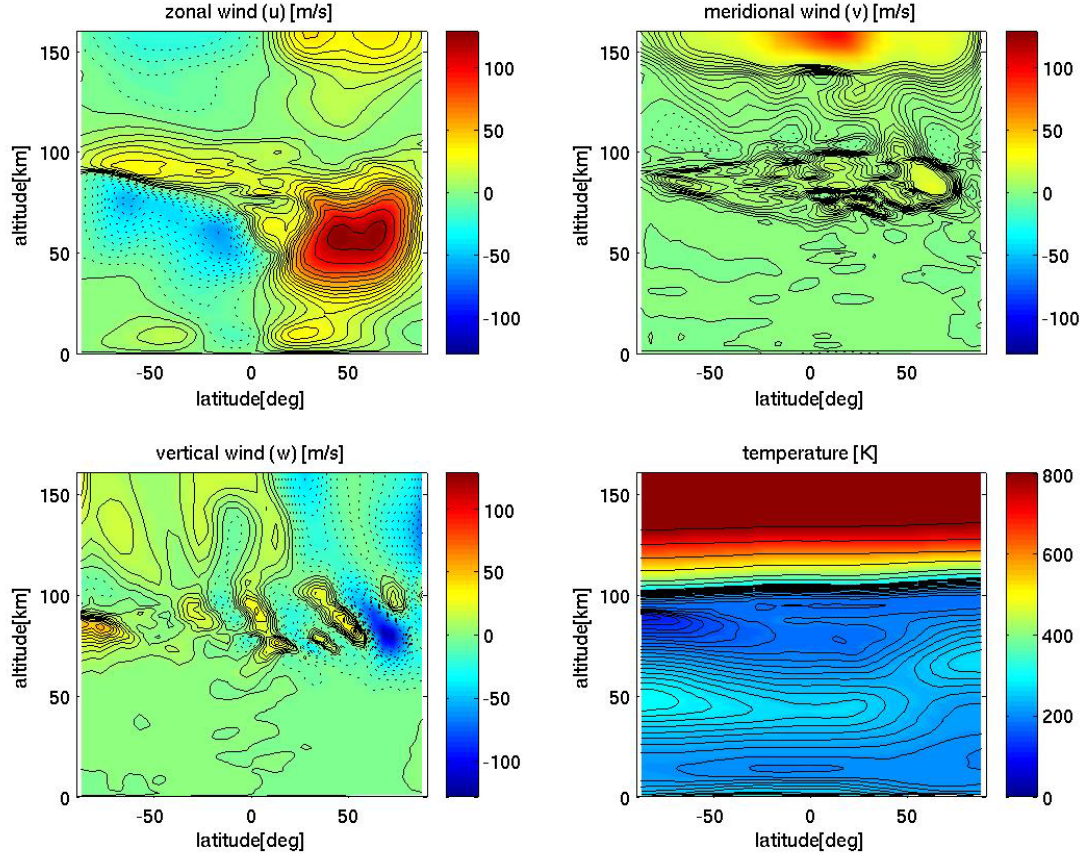


Figure 6. Atmospherical data.

On the first map, the strong zonal wind appearing during summer is visible and whereas during winter (in the south hemisphere) the zonal wind is more smooth and of lower speed. It can be also observed on the temperature map that the stratopause height varies a lot with the latitude. In addition to these mean values, the IAP provides also simulated data of atmospheric gravity waves. They correspond to finer length scale inhomogeneities of the atmosphere and their influence is investigated by adding them to the mean atmospheric fields. These data have to be interpolated over the whole propagation domain. This is performed by using third-order polynomials as continuity has to be preserved up to the second spatial derivatives of the fields.

VI. Sonic boom signatures for realistic atmospheric conditions

In this part we present some of the results obtained by using the code describes in the previous section. In a first part, the primary sonic boom results are presented. The initial conditions are characteristics of a Concorde flying at a Mach 2 speed. The aircraft is located at a latitude of around 45 degrees North for

summer atmospheric conditions. It has been point out that the secondary sonic boom is reflected in the thermosphere or in the stratopause and this leads to two different kinds of secondary sonic boom. The two differents situations are tested in this section. In the second part, the aircraft position is chosen such that the maximum wind velocity at stratopause altitude is 60 m.s^{-1} . For this velocity, the upper part of the Mach surface is reflected in the thermosphere. In the figure 7, this corresponds to the thermospheric ray plotted as a blue curve. In the third part, the maximum wind velocity at stratopause altitude is 80 m.s^{-1} . For that case, the entire Mach surface is reflected at stratopause altitudes (50 km). This stratospheric ray is plotted with a red curve in figure 7.

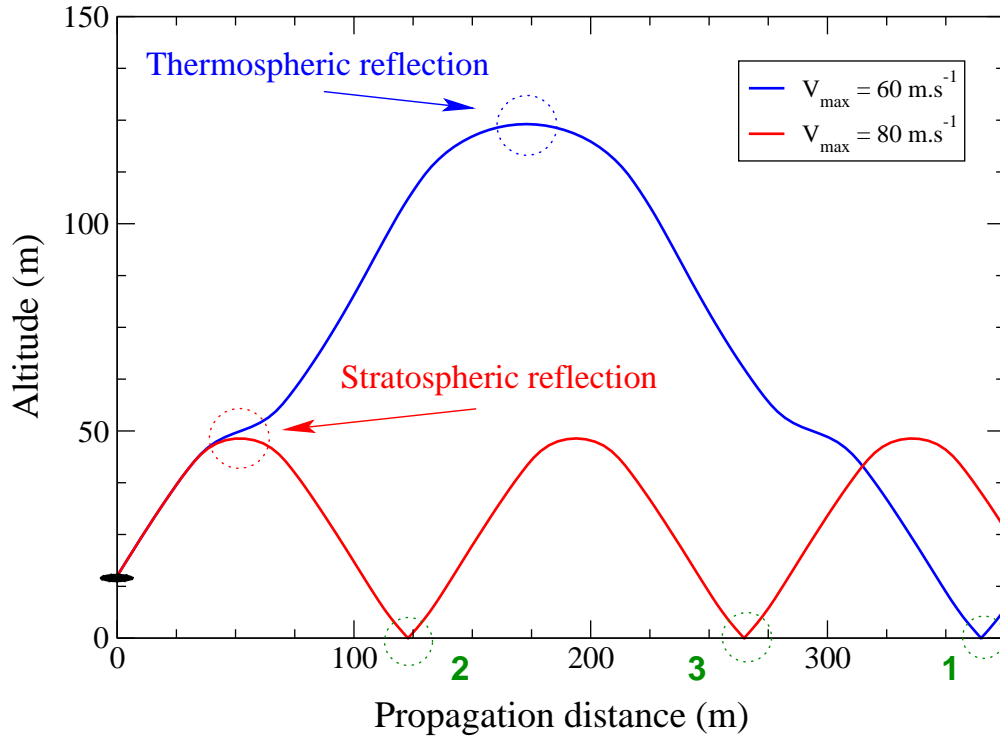


Figure 7. Thermospheric and stratospheric rays.

A. Primary sonic boom

The figure 8 presented the primary sonic boom signature calculated with the model presented in this paper. The atmospheric data are averaged over a day and it was not the purpose of this work to study in details the effect of the lower layer of the atmosphere (1 km over the ground). So, the primary boom signature is relatively unrelated for this model to the aircraft position or direction. The both graphs of the figure 8 compare the primary boom signature (red plain line) to the initial condition (blue dashed line) for the launching angle $\theta = 0$. The left graph shows the pressure level of the primary sonic boom and the right graph shows the undimensionnalize u function. The peak pressure level of the primary sonic boom is around 50 Pa. This is in accordance with the values recorded in the litterature. The peak pressure amplitude is reduce by ten during the propagation from the aircraft to the ground. However most of the decrease is due to the variations of the underlying atmophere. The amplitude of the u function which keeps only the absorption, relaxation and nonlinear effects is just divided by two. Concerning the surface under the curve, it remains mostly constant. This means that the dominant effect at these altitudes is the nonlinearity.

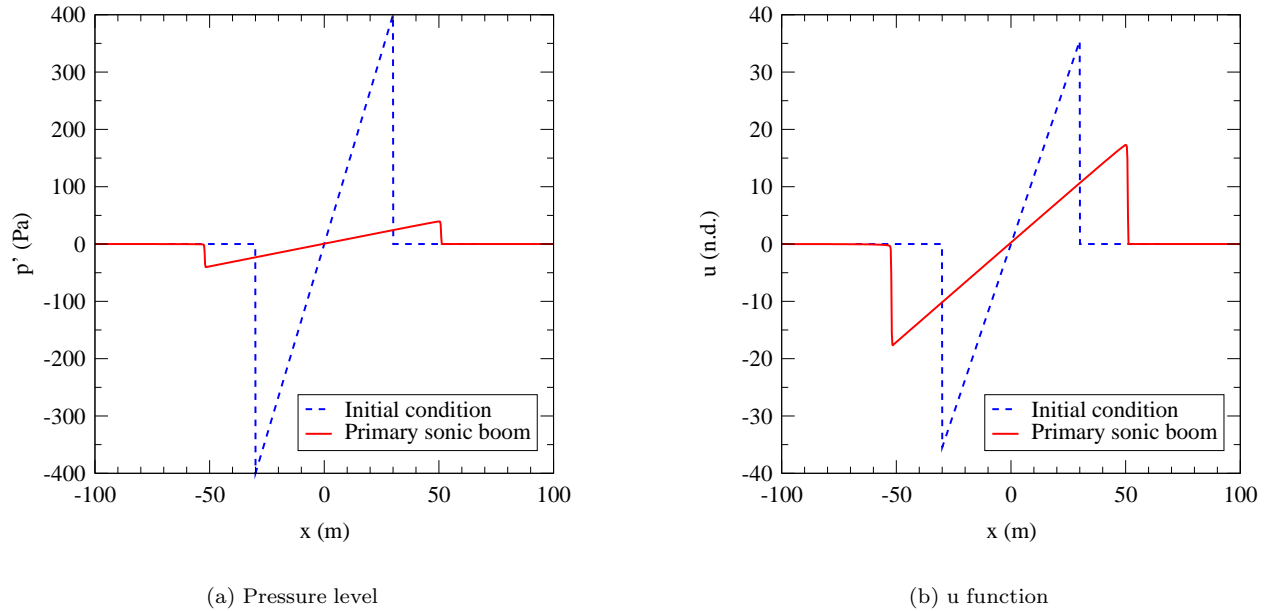


Figure 8. Primary boom

B. Secondary boom signatures

The annoyance from sonic booms is concentrated at the carpet position where the Mach surface is reflected by the ground. The primary carpet due to the primary sonic booms that travel directly downward the ground are unaffected by the gravity waves. The secondary sonic booms which travel in the upper part of the atmosphere before being reflected back to the ground are more dependent on the atmospheric structure.

Considering the mean atmospheric sound speed, two waveguides exist for the boom rays. The thermosphere is the upper boundary of the first waveguide. Most of the boom rays trapped in this waveguide reach the ground. As a large part of the boom ray is at altitudes (over 50 km) where absorption and relaxation are the dominant effects, the secondary boom signature is an infrasonic signal (cf. figure 9(a)). Due to its low frequency, this wave can travel over very long distances in the atmosphere. The peak pressure amplitude is around 0.1 Pa and the frequency is around 0.05 Hz. These values are in accordance with long distance measurements of secondary boom.^{3,4}

The second waveguide is between the stratopause and the troposphere. As the maximum sound speed in the stratopause is less than the sound speed at ground level, boom rays trapped in this waveguide reach the ground only if the shock wave is appropriately convected by wind at the reflection altitude (around 50 km). The resulting secondary sonic boom signature has a higher amplitude than the thermospheric one with a peak pressure amplitude of 4 Pa (cf. figure 9(b)). Its frequency is also much higher (0.5 Hz) and shocks persist. These values are also in agreement with some measurements of secondary sonic boom.⁵

C. Influence of gravity waves

The primary influence of the gravity waves on the secondary sonic booms concerns the secondary carpets. The methodology for creating an upper atmosphere model with a realistic gravity wave structure consists of using observed spectral amplitudes and theoretical linear mode shapes to put together a random spatial field (of wind, temperature, pressure and density perturbations) that has the correct physical nature and realistic

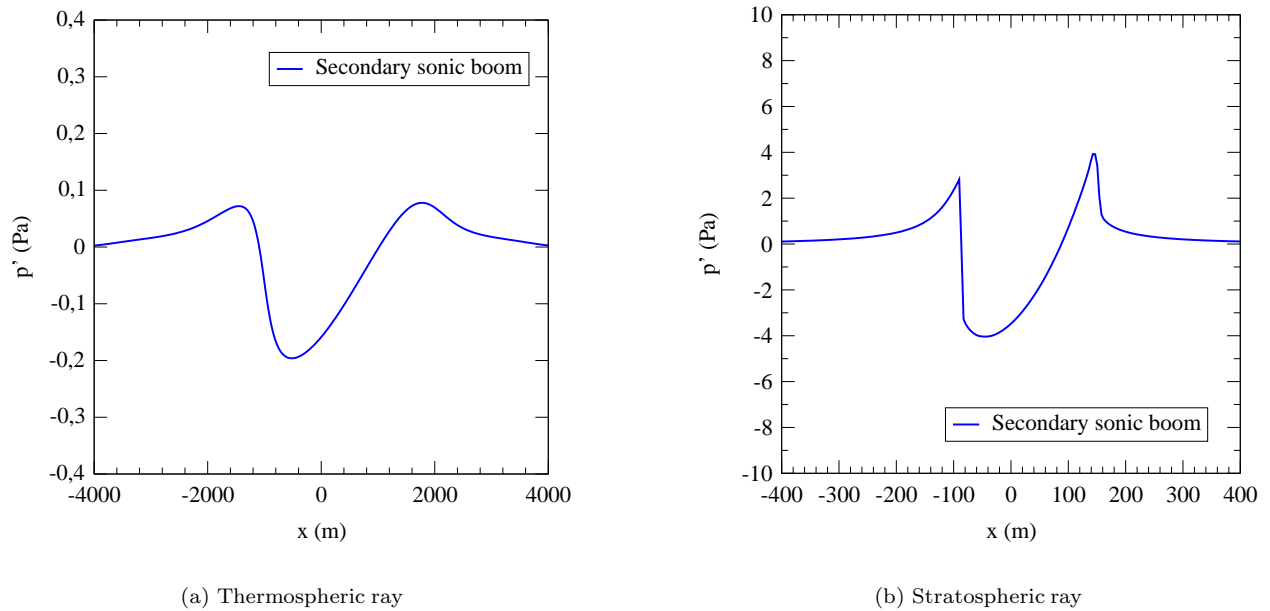


Figure 9. Secondary boom signatures predict by the model.

statistical properties. This involves also applying realistic breaking criteria for convective and dynamic instabilities. Because the boom ray equations involve second derivatives of the underlying atmospheric fields, a sufficiently smooth interpolation has to be performed on the atmospheric data in order to use it, and we have done this using cubic polynomials (in order to provide continuous second derivatives).

The figure 10 compares the secondary sonic boom carpets when the atmospheric data do or do not contain gravity waves. The figure 10(a) is obtained when gravity waves are not included to atmospheric data. The leftmost carpet corresponds to the primary boom. The two carpet patches at a medium distance from the aeroplane ($x \sim 150$ km) are created by boom rays reflected by the stratopause. The last carpets ($x \sim 300$ km) are due to the thermospheric boom rays. Each carpet is composed of a direct and an indirect part, the indirect part being due to the rays reflected back to the atmosphere from the primary carpet position. The distance between the direct and the indirect secondary carpet is around 20 km. This is in agreement with the time duration between the bursts of secondary sonic boom (around 30 s). The carpets are smooth and a clear difference appears between each one.

The figure 10(b) is obtained when gravity waves are included. The primary carpet is not influenced by the gravity waves. The gravity wave influence appears on the secondary carpet geometry. The secondary carpets look more complex and the direct and indirect secondary carpets cannot be distinguished anymore. A greater number of rays reaches a given earth location. It may be expected that it is the main reason of the rumble noise.

Conclusion

The present results show that the signature model predicts well the amplitude and the frequency of the secondary sonic booms. The rumble noise and the bursts may be explained by multipath arrivals of secondary sonic booms. The bursts seem to be linked to the arrival of direct and indirect rays and the rumble noise to the presence of gravity waves or other fine scale effects in the atmosphere.

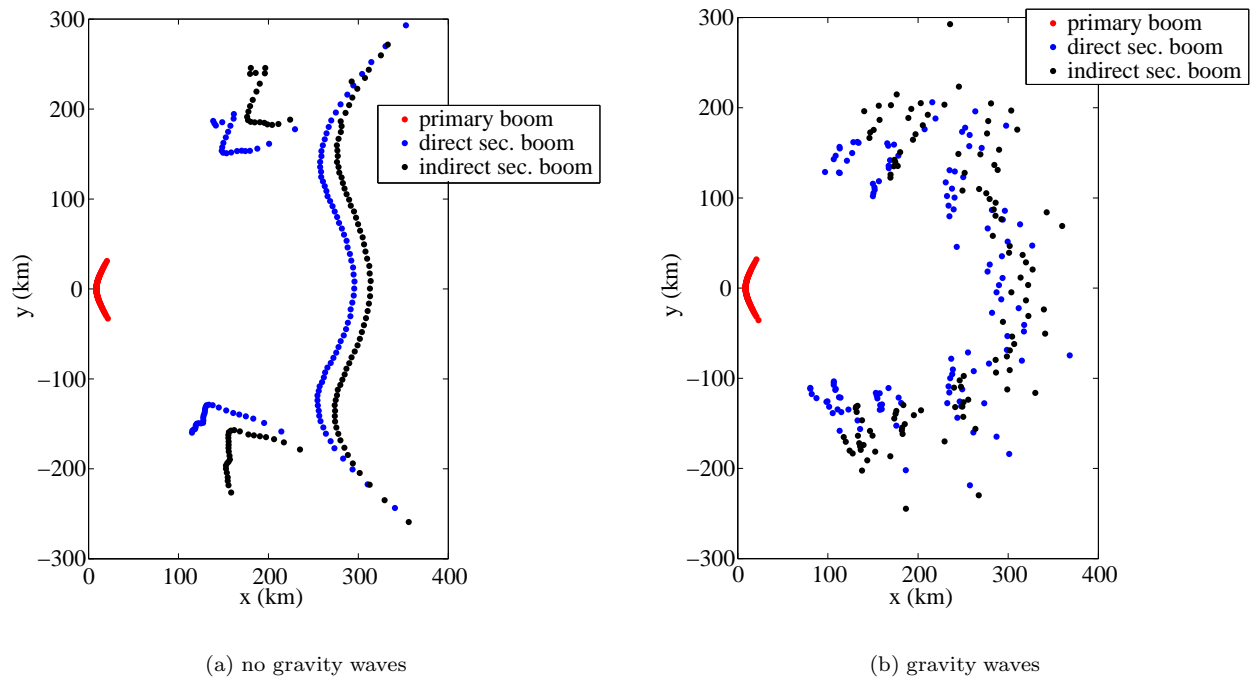


Figure 10. Secondary boom carpets for realistic atmosphere

Acknowledgments

This work is supported by the European Community (*SOBER* project, Contract No. G4RD-CT-2000-00398).

References

- ¹ROGERS, P. H. & GARDNER, J. H., 1980, Propagation of sonic booms in the thermosphere, *J. Acoust. Soc. Am.* **67**, 78-91.
- ²HAGLUND, GEORGE T. & POLING, HUGH W., 1995, HSCT sonic boom impact at the earth's surface due to secondary booms, Tech. Report Boeing Commercial Airplane Company.
- ³GROVER F. H., 1973, Geophysical effects of Concorde sonic booms, *Quart. J. Roy Astron. Soc.*, **14**, 141-160.
- ⁴LISZKA LUDWIK, 1978, Long-distance focusing of Concorde sonic boom, *J. Acoust. Soc. Am.* **64**, 631-635.
- ⁵RICKLEY, E. J. AND PIERCE, A. D., 1980, Detection and assessment of secondary booms in New England, Technical Report FAA-AEE-80-22.